NASA DEVELOP National Program
Georgia – Athens
Fall 2021

Peru Health and Air Quality II

Leveraging Earth Observations and Health Data to Map Outbreak Risk and Inform Public Health Interventions for Zoonotic Disease Prevention

DEVELOP Technical Report
Final – November 18th, 2021

Jennifer Rogers (Project Lead)
Melanie Cabrera
Gayatri Girirajan
Julianne Liu

Advisors:
Dr. Marguerite Madden, University of Georgia, Center for Geospatial Research (Science Advisor)
Dr. Xiao Feng, Florida State University (Science Advisor)

Previous Contributors:
Elizabeth Stapleton
Ariel Calle
Nataly Chacon
Nelson Huffaker
Oliver Nguyen

1. Abstract

Peru's Madre de Dios region is a hotspot for dengue fever and leishmaniasis due to its tropical Amazonian climate. Though treatable, these zoonotic diseases are debilitating for under-resourced communities whose already close proximity to mosquito and sandfly vectors continues to increase via rapid urbanization and deforestation. Peru's Ministries of Health (MINSA) and Environment (MINAM) are working to better understand the environmental factors amplifying the risk of dengue fever and leishmaniasis transmission. The first term of this project classified the land use and land cover of Madre de Dios' 11 districts for 2010, 2015, and 2020 and identified a correlation between both diseases and urbanization. Our team expanded this analysis by creating urban-forest edge maps and incorporating climatic and topographic variables with data from Landsat 7 Enhanced Thematic Mapper Plus (ETM+), Landsat 8 Operational Land Imager (OLI), the Global Precipitation Measurement (GPM) Integrated Multi-satellitE Retrievals for GPM (IMERG), and the Shuttle Radar Topography Mission (SRTM). We determined these variables' impacts on disease incidence by assessing existing literature and running regression models. Dengue fever correlated with urban-forest edge, urban area, slope, temperature, and precipitation. Leishmaniasis primarily correlated with forest-edge area and elevation, but lacking additional statistical significance prevented further work, a decision supported by the literature. Thus, the risk matrix and risk map which we scripted in R to visualize the risk of disease posed to districts alongside health post locations addresses only dengue fever. The results and products will inform MINSA and MINAM in public health interventions, resource distribution, and policy initiatives.

Key Terms

Madre de Dios, South America, dengue fever, leishmaniasis, risk matrix, risk map, remote sensing, land use

2. Introduction

2.1 Background Information

Madre de Dios is a biodiverse region of 11 districts located in the Peruvian Amazon (*Figure* 1, *Figure* 2). The tropical rainforest climate makes it a hotspot for dengue fever and leishmaniasis, two zoonotic diseases endemic to Peru. Dengue fever is spread by the yellow fever mosquito, *Aedes aegypti,* which breeds in damp urban environments (Guagliardo et al., 2015). Leishmaniasis is transmitted by *Psychodidae* sandflies in forest settings and city-forest borders, especially in areas with inadequate sanitation (World Health Organization, 2021). Rural, indigenous communities like the Awajún, Wampís, and Achuar report high contraction from hunting in remote areas (K. Hopfgartner, personal communication, October 17, 2021). Continued rural development has further disrupted these insects' habitats and contact between humans and disease vectors have been rapidly increasing. Our team examined district-level climatic and topographic data from 2010 and 2020 with additional land use land cover (LULC) information for 2010, 2015, and 2020 to understand the region's risk of dengue fever and leishmaniasis.

Figure 1. Study area of Madre de Dios, Peru.

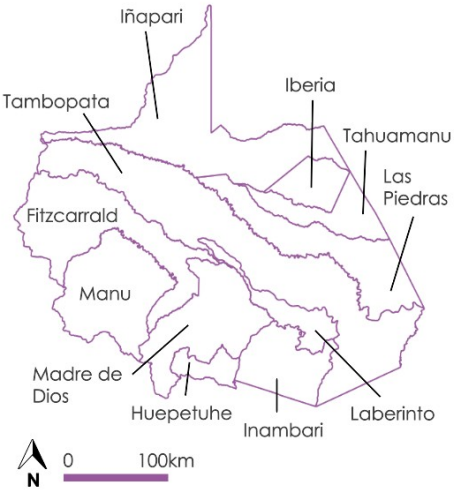

Figure 2. The 11 districts in the region of Madre de Dios.

Risk of zoonotic disease transmission is intimately linked with environmental variables. For example, dengue fever vectors are more active in warmer temperatures and the wet season, while leishmaniasis vectors rely on low seasonal variation for high transmission (Charette et al., 2020; Purse et al., 2017). Elevation is also a key determinant. Chowell et al. (2008) found that dengue fever rarely occurs below 1,500 meters, and Purse et al. (2017) identified elevation as the most important landscape predictor of cutaneous leishmaniasis. Moreover, land use change greatly contributes to the risk of zoonotic disease outbreaks. Madre de Dios has experienced an average forest loss of 4,128 ha per year since the construction of the Interoceanic Highway in 2011 (Nicolau et al., 2019). Much of this deforestation has been followed by gold mining and agriculture, which operate near rivers and rural forest fragments in which sand flies thrive, increasing the potential for human-vector interaction (Borges et al., 2015). Additionally, rural-urban nodes like the Interoceanic Highway facilitate dengue transmission (Salmón-Mulanovich et al., 2018), and population density further amplifies risk. Previous studies have analyzed the effects of environmental variables on zoonotic disease transmission. Using a stepwise regression model and time series analysis, Chowell et al. (2008) found a positive relationship between precipitation, temperature, and disease incidence in Peru. Another study used a Spearman's rank analysis to correlate dengue fever incidence and population size in Europe to create a predictive model (Salami et al., 2020). These methods informed our project and guided the analysis of multiple environmental variables to create a model assessing disease risk.

Over two terms, the Peru Health and Air Quality project worked to uncover the relationship between zoonotic disease incidence and climatic, topographic, and land use land cover variables in Madre de Dios. Term I integrated satellite imagery from Landsat 5 Thematic Mapper (TM) and Landsat 8 Operational Land Imager (OLI) into a LULC classification script in Google Earth Engine (GEE). They produced raster maps for 2010, 2015, and 2020 and quantified the results by total area and percent change, ultimately finding a correlation between urbanization (km^2) and total dengue fever and leishmaniasis incidence. Our team integrated the

LULC assessments into our expanded analysis of climatic and topographic variables influencing dengue fever and leishmaniasis incidence.

2.2 Project Partners and Objectives

The Peruvian Ministry of Health (Ministerio de Salud, MINSA) and Ministry of Environment (Ministerio del Ambiente, MINAM) were interested in exploring applications of remote sensing to address zoonotic disease outbreaks in Madre de Dios. MINSA regulates the national healthcare system, monitors diseases, and conducts outreach for preventative care. MINAM oversees matters relating to biodiversity and land conservation. Both ministries partnered with our NASA DEVELOP team to identify districts vulnerable to outbreaks of dengue fever and leishmaniasis. We also received additional technical support, cultural context, and satellite imagery from the Lab for EcoHealth and Urban Ecology at la Universidad Peruana Cayetano Heredia, La Asociación para la Conservación de la Cuenca Amazónica (ACCA), El Instituto del Bien Común (IBC), and La Comisión Nacional de Investigación y Desarrollo Aeroespacial (CONIDA).

We assisted MINSA and MINAM in determining the degrees of vulnerability for each district in Madre de Dios. We scripted disease outbreak risk matrices in R to correlate disease incidence in relation to climatic, topographic, and LULC variables. Our R script further maps risk alongside the current distribution of local medical centers, known as health posts, to emphasize the location of resources compared to risk. To increase public awareness about zoonotic disease in the region, we also recorded the project's methodology and results in a video narrated in both English (https://youtu.be/z1C5YwoQYG0) and Spanish (https://youtu.be/gov429G5CK0). Ultimately, MINSA and MINAM can utilize the risk matrix, risk maps, and video, alongside the products from Term I, to identify which districts could benefit from public health interventions, expanded healthcare infrastructure, and designated protected land. These products can also support advocacy for best practices in urban planning, public sanitation, and resource management.

3. Methodology

3.1 Data Acquisition

We used GEE to visualize and export temperature data from Landsat 7 Enhanced Thematic Mapper Plus (ETM+) and Landsat 8 OLI, precipitation data from the Global Precipitation Measurement (GPM) Integrated Multi-satellitE Retrievals for GPM (IMERG), and elevation and slope from the Shuttle Radar Topography Mission (SRTM; Table 1). We used GEE scripts developed during the first term of the project to obtain information on LULC classes created using Landsat 5 TM and Landsat 8 OLI imagery (Stapleton et al., 2021). Ancillary datasets provided data for all other variables (Table 2). MINSA supplied weekly zoonotic disease incidence reports which were organized to display dengue fever and leishmaniasis cases originating in districts within Madre de Dios. To normalize disease incidence, we acquired population data for 2010 and 2020 from Term I's interpolation of 2007 and 2017 census data from the Peruvian National Institute of Statistics and Informatics. Additionally, we downloaded health post points from Geo Perú's Plataforma Nacional de Datos Georreferenciados. Lastly, information from Geoservidorperu (Sideteva) was also used during the first term of the project to help define mining areas while completing the LULC classification.

Table 1
Earth Observation products, accompanying resolutions, and the derived variables

Satellite and Sensor	Parameters	Spatial Resolution (meters)	Years	Source	Variable
Landsat 5 TM	Surface Reflectance, Tier 1; Normalized Difference Vegetation Index (NDVI); Normalized Difference Water Index (NDWI); Enhanced Vegetation Index (EVI)	30 m	2010	GEE	LULC
Landsat 7 ETM+	Surface Reflectance, Tier 2; Temperature	30 m	2010-2014	GEE	Temperature
Landsat 8 OLI	Surface Reflectance, Tier 2; Temperature; NDVI; NDWI; EVI	30 m	2015-2020	GEE	Temperature & LULC
GPM IMERG	Precipitation, Version 6	11,000 m	2010-2020	GEE	Precipitation
SRTM Digital Elevation Data	Digital Elevation Model, Version 4	90 m	2000	GEE	Elevation & Slope

Table 2
Ancillary Datasets

Dataset	Years	Source	Variable
Weekly Disease Incidence Reports	2000-2021	MINSA	Disease Incidence
Health Post Points	2021	Geo Perú's Plataforma Nacional de Datos Georreferenciados	Health Post Locations

Census Data	2007 & 2017	Peruvian National Institute of Statistics and Informatics	Population

3.2 Data Processing

3.2.1 Addressing Seasonality

Our team sought to better understand the complex interactions between environmental factors, disease incidence, and seasonality as dengue fever and leishmaniasis transmission varies over the course of the year. Additionally, some literature suggests a lag period five weeks following climatic conditions to time of infection, identified by Chowell et al. (2008) for dengue fever. To address these nuances impacting the risk of dengue fever and leishmaniasis, we organized temperature and precipitation data into seasons to compare these variables to disease incidence for a particular season. Informed by partners and meteorological reports, we classified the wet season as November to March and the dry season as April to October. With a span of five and seven months, respectively, these seasonal metrics better encompassed effects of a lag period. While the wet season remained an individual variable, we integrated the dry season into a new variable —seasonal year—which encompassed both wet and dry seasons from November to October. This merge was due to significant gaps in the satellite data for temperature during the dry season, potentially caused by sensor and coding errors. We chose to use the term seasonal year to distinguish that our period was November to October, rather than the typical calendar year of January to December which could be conveyed by “annual incidence.” We organized our health data to follow the same pattern. With dengue fever and leishmaniasis incidence reported at the weekly level, we calculated the total cases which occurred in the wet season and the seasonal year for both diseases. We executed all of these steps in R Studio, which we extensively utilized throughout our project to organize, analyze, and visualize our data.

3.2.2 Climatic and Topographic Variables

For temperature, we used the GEE interface to clip the Landsat 7 ETM+ and Landsat 8 OLI datasets to the 11 districts within the Madre de Dios region and filtered the wet and dry seasons for 2010, 2015, and 2020. We then organized our data according to the wet season and seasonal year. After converting temperature from Kelvin to Celsius to align with the metrics used in Peru, we applied the same clipping, filtering, and visualization process for precipitation, elevation, and elevation-derived slope. For each of these climatic and topographic datasets, we extracted the minimum, maximum, mean, and median values aggregated to the district level. Then, these data were imported into R, where we formatted each to include just the parameter value, removing superfluous information about the system index and identification numbers. We also calculated an additional metric of range in R by subtracting minimum values from maximum values.

3.2.3 LULC Variables

The LULC data we obtained from the previous term contained eight classes (urban, forest, secondary vegetation, mining, agriculture, pasture lands, water, and wetlands), but we removed secondary vegetation due to our focus on the other categories identified as common areas for human-vector interaction. Scientific literature has consistently identified urban areas as important for dengue fever

transmission and forested areas for leishmaniasis transmission. Thus, we retained urban and forest as individual LULC variables. Food production and wet environments are also proven vector breeding grounds and places of human-vector interactions (Lana et al., 2021; Tsheten et al., 2021; Yanoviak et al., 2006). To explore this pattern in our data, we grouped agriculture and pasture lands into one variable and water and wetlands were grouped into another. We also created another variable which combined urban, mining, agriculture, and pastureland to explore the significance of human-altered environments. The final LULC variables used in the project were (1) urban, (2) forest, (3) agriculture and pastures, (4) water and wetlands, and (5) human-altered environments (urban, mining, agriculture, and pastures). All data were measured by total area (km^2), and from this metric we calculated proportion of the total district area (%).

We further processed our raw LULC data to calculate urban, forest, and urban-forest edges due to their importance in harboring vectors. Dengue-carrying mosquitoes are prevalent in microhabitats created by recent deforestation (Yanoviak et al., 2006). The first term of this project also noted that a large number of leishmaniasis cases occurred in Manu, a rural area undergoing high rates of deforestation. We adapted the methodology of Gambino et al. (2019), who studied tick-borne disease in Maine, to calculate the overlapping urban-forest edges in GEE using our LULC maps of Madre de Dios. This method uses Euclidean distance to calculate the distance within 30 meters for both urban and forest cover edges and then creates a buffer along edges using the focalmax and after which calculates the areas of overlap between forest and urban edge. The pixels and subsequent area for the three separate layers (i.e., forest edge, urban edge, and forest-urban edge) were counted as total raw values (km^2) and as the percent area in each district (%).

3.3 Data Analysis

3.3.1 Statistical Analysis

We first evaluated the correlations between variables within the climatic, topographic, and LULC variable categories for each disease for the wet season and seasonal year in 2010 and 2020 (Appendix A). We applied a Spearman's rank correlation on our variables because it is a nonparametric test which does not assume normal distribution or linear relationships and is suitable for a small sample size. This process identified the correlated and collinear intra-categorical variables, which subsequently informed our primary statistical analysis that used multivariable regression models. In the case that two variables were highly corelated with each other, we selected one to avoid redundancy in our multivariable regression models.

After checking correlation and collinearity, we assessed our dependent variables for normality (the distribution of the data) and heteroskedasticity (the unequal variance of residuals) with the Shapiro-Wilks test and diagnostic plots to verify that our data met the assumptions of linear and stepwise regressions. We then ran stepwise and linear regression models for the wet season and seasonal year in 2010 and 2020 to determine the most appropriate climatic, topographic, and LULC variables for estimating disease incidence. Using the R stats package, we ran models with individual variables against disease incidence. Next, to build the strongest models, we used individual models to down select variables for a final

model, integrating the variable with the strongest R^2 and p-value in each category. We also chose variables which had an established association with each disease, regardless of statistical significance in our tests. The most explanatory individual variables (high R^2 and low p-value) informed our likelihood axis in the risk matrix and risk map. The most explanatory multivariable models highlighted which individual variables held the greatest significance among the climatic, topographic, and LULC categories. From dengue fever models, we found urban area, urban-forest edge area, slope range, and precipitation range to be most effective. For leishmaniasis, forest edge area and elevation mean were important.

3.3.2 Risk Matrices and Risk Maps

To visualize each district's risk, we created a script which generates risk matrices and risk maps in R. In the risk matrix, districts were organized with respect to their levels of risk as a product of likelihood and population, categorized from very low to very high risk. We built the likelihood axis from the results of our regression analyses, partners' expertise, and scientific literature. Each variable contributing to likelihood was divided into four intervals based on quantiles and assigned a value between one, very low risk, and four, very high risk. We further assigned weights to variables based on the strength of their impact on disease transmission which was influenced by expert opinion. The weighted mean of these variables was then taken to calculate the overall likelihood parameter.

The population axis represents consequence of disease transmission. With varying population density across Madre de Dios, the population parameter considers which districts have the higher potential for disease spread based on the number of people who can be infected. Population parameter intervals were also determined by the quantile of population values from 2007 to 2020. Points on the risk matrix represent individual districts in their overall risk, and as new data for subsequent years are input into the matrix, these points will move accordingly. To allow for these iterations, we incorporated linear interpolations for population using 2007 and 2017 census data and ultimately urban-forest edge and urban area using 2010 and 2020 LULC data. The script also includes the option for users to input updated data. To accompany the risk matrix, we created a script for risk maps which geographically visualize each district's level of risk in the form of a choropleth map, where the colors of districts correspond with the risk assigned in the matrix. Additionally, we overlaid the current distribution of health posts to portray the level of risk compared to resources.

4. Results & Discussion

4.1 Regression Results

4.1.1 Stepwise and Linear Regression

In meeting the assumptions of stepwise and linear regression, the distribution of dengue fever data was near-normal for the wet season and seasonal year in 2010 and 2020. In the Shapiro-Wilk test, dengue fever yielded normal p-values between 0.0489 and 0.145. Leishmaniasis data, however, did not yield the same normality. Only seasonal year 2010 displayed normality. Due to our small sample size (n=11) which may have obscured normality, we exercised extreme caution in reading results for leishmaniasis in our regression analyses.

In stepwise regression, the combinations of independent variables selected by the model were often correlated, weakening the efficacy of this model. Moreover, whereas the stepwise regression consistently produced results for dengue fever, this model yielded few results for leishmaniasis. We found greater success with linear regression models, though only with dengue fever, detailed below.

4.1.2 Dengue Fever Results

Urban area, urban-forest edge area, slope range, and precipitation range were the individual variables from each category which best explained dengue fever incidence across all years (Table 3). Even when linear regression assigned no statistical significance, these selected variables remained the most explanatory for that year and season compared to the other variables in their respective categories. Partner expertise and patterns in scientific literature also affirmed the importance of these variables. Urban areas and urban-forest edge areas foster habitats for mosquitoes and human-vector interaction. Precipitation range is also a logical explanatory variable as water is needed for vector breeding, but too much precipitation could destroy vector habitats. Slope range requires more interpretation but was presumably strongly correlated because slope impacts water retention and is strongly tied to elevation and thus climate. Temperature was notably omitted from our selected variables of importance, despite it being a known influencing factor for dengue fever vector survival and subsequently transmission. An error identified in our data acquisition process at this stage led us to discard the use of temperature in our regression models, risk matrices, and risk maps.

Table 3
Dengue Fever Regression Results: Individual Variables.
*(** indicates statistical significance at the 1% level, * at the 5% level, and • at the 10% level)*

Variable	Wet Season 2010		Seasonal Year 2010		Wet Season 2020		Seasonal Year 2020	
Urban Area (km^2)	$R^2 = 0.3725$		$R^2 = 0.3628$		$R^2 = 0.1681$		$R^2 = 0.1763$	
	$\rho = 0.0272$	*	$\rho = 0.02934$	*	$\rho = 0.1162$		$\rho = 0.1101$	
Urban-Forest Edge Area (km^2)	$R^2 = 0.5389$		$R^2 = 0.5536$		$R^2 = 0.2235$		$R^2 = 0.2167$	
	$\rho = 0.006$	**	$\rho = 0.005229$	**	$\rho = 0.08044$	•	$\rho = 0.08422$	
Slope Range	$R^2 = 0.4059$		$R^2 = 0.4023$		$R^2 = 0.4704$		$R^2 = 0.4587$	
	$\rho = 0.02076$	*	$\rho = 0.02138$	*	$\rho = 0.01186$	*	$\rho = 0.01318$	*
Precipitation Range (mm)	$R^2 = 0.3153$		$R^2 = 0.3084$		$R^2 = 0.06715$		$R^2 = 0.05632$	
	$\rho = 0.04209$	*	$\rho = 0.04427$	*	$\rho = 0.2222$		$\rho = 0.2381$	

Overall, the ability of these variables to explain dengue fever incidence was stronger in 2010 than 2020. We cannot definitively attribute this trend to any variables, but it may have been influenced by climatic variation and long-running factors such as land use change and migration patterns. Dengue fever incidence in

2020 may have also been affected by the COVID-19 pandemic changing the interactions among humans and between humans and vectors. Additionally, the differences between wet season and seasonal year were often minor, a logical result as most dengue fever cases occur in the wet season. An extended table of regression results for each variable is available in Tables B1, B2, B3, and B4.

After identifying these individual variables as important, we ran multivariable linear regression to explore which combinations were most predictive of dengue fever incidence. We built our models around the most significant individual variables and variables identified as important from the scientific literature. In most cases, the model did not greatly improve from the results of the strongest individual variable: urban-forest edge area. While these models were informative for our own understandings, the significance of individual variables was most important to our project.

4.1.3 Leishmaniasis Results

Of all the individual variables analyzed against leishmaniasis incidence, slope and elevation metrics were the only ones to display statistical significance in linear regression. Metrics were often correlated, though elevation mean had the most explanatory abilities. The expected variables addressing human-forest interaction yielded low, and even negative, R^2 values and high p-values (Table 4). We found this pattern across the other LULC and climatic variables as well (Tables C1, C2, C3, and C4). Multivariable linear regression models for leishmaniasis were similar to those run for dengue fever in that combinations did not greatly improve the results from the strongest independent variable. Notably, though, using forest edge in combination with elevation mean yielded the best performing model with an R^2 of 0.8027 and p-value of 0.000621.

Table 4
Leishmaniasis Regression Results: Individual Variables.
*(*** indicates statistical significance at the 0.1% level and ** at the 1% level)*

Variable	Wet Season 2010		Seasonal Year 2010		Wet Season 2020		Seasonal Year 2020	
Elevation Mean	$R^2 = 0.7461$		$R^2 = 0.7387$		$R^2 = 0.6239$		$R^2 = 0.5015$	
	$\rho = 3.74x10^{-4}$	***	$\rho = 4.27x10^{-4}$	***	$\rho = 2.33x10^{-3}$	**	$\rho = 8.86x10^{-3}$	**
Forest Area (km^2)	$R^2 = -0.07692$		$R^2 = -0.0794$		$R^2 = -0.1001$		$R^2 = -0.08193$	
	$\rho = 0.6059$		$\rho = 0.6175$		$\rho = 0.7705$		$\rho = 0.634$	
Forest Edge (km^2)	$R^2 = 0.05229$		$R^2 = 0.04496$		$R^2 = 0.07705$		$R^2 = -0.03265$	
	$\rho = 0.2443$		$\rho = 0.2561$		$\rho = 0.2086$		$\rho = 0.4296$	
Urban-Forest Edge (km^2)	$R^2 = -0.07998$		$R^2 = -0.02922$		$R^2 = 0.06285$		$R^2 = 0.05536$	
	$\rho = 0.6228$		$\rho = 0.4193$		$\rho = 0.2284$		$\rho = 0.2396$	

Other researchers have also encountered difficulty in working with leishmaniasis. Okwor and Uzonna (2016) explained the concentration of leishmaniasis in rural places and the limited access to healthcare facilities. In their review of leishmaniasis in Latin America, Romero and Boelaert (2010) discussed the lack of studies to control leishmaniasis vectors and the urgent need for researchers to prioritize the disease. Moreover, some of our partners noted the under-reporting and under-researching of the disease. Ultimately, we decided to proceed without leishmaniasis for our risk matrices and risk maps due to the limited statistical significance of our regression analyses, supporting literature about the difficulties of modeling leishmaniasis, and experiences of our partners.

4.2 Risk Matrix and Risk Map Results

Using the significant variables identified as important in our regression analyses and validated by partners, we created risk matrices for dengue fever. In our likelihood parameter, we used, in order of importance and assigned weight: urban-forest edge area (km^2), urban area (km^2), precipitation range (mm), and slope range. Additionally, we coded a framework to incorporate temperature minimum based on the values reported in the scientific literature.

Risk matrices and maps were created for 2010 and 2020 and reviewed for their accuracy compared to incidence data. In particular, there was a shift from 2010 to 2020 to higher disease incidence that is reflected in a shift to higher risk (*Figure* 3, *Figure* 4, Table 5). Moreover, we found that assigning weight to variables according to expert opinion better matched a district's level of risk to its total disease incidence, compared to the performance of risk matrices built with unweighted means. Overall, for the 2010 and 2020 matrices, districts with high and low levels of risk compared well to total disease incidence (Table 5).

The role of increasing urban-forest edge area can be seen in districts such as Tambopata. In 2010, Tambopata had urban area in the very high category and precipitation range also in the very high category, leading to an overall classification of the district as one with somewhat high likelihood. Because Tambopata also has the highest population, it was assigned at high risk of transmission. In 2020, Tambopata doubled its urban-forest edge area. This increase shifted the district to higher likelihood and subsequently at very high risk for transmission. Inambari in 2020 had the largest area of urban-forest edge after undergoing an order of magnitude increase in its urban-forest edge area. Because of this change, it advanced from somewhat high to very high disease risk. Matrices were also depicted more intuitively in map format, the shift to red shades from 2010 to 2020 is apparent (*Figure* 5, *Figure* 6).

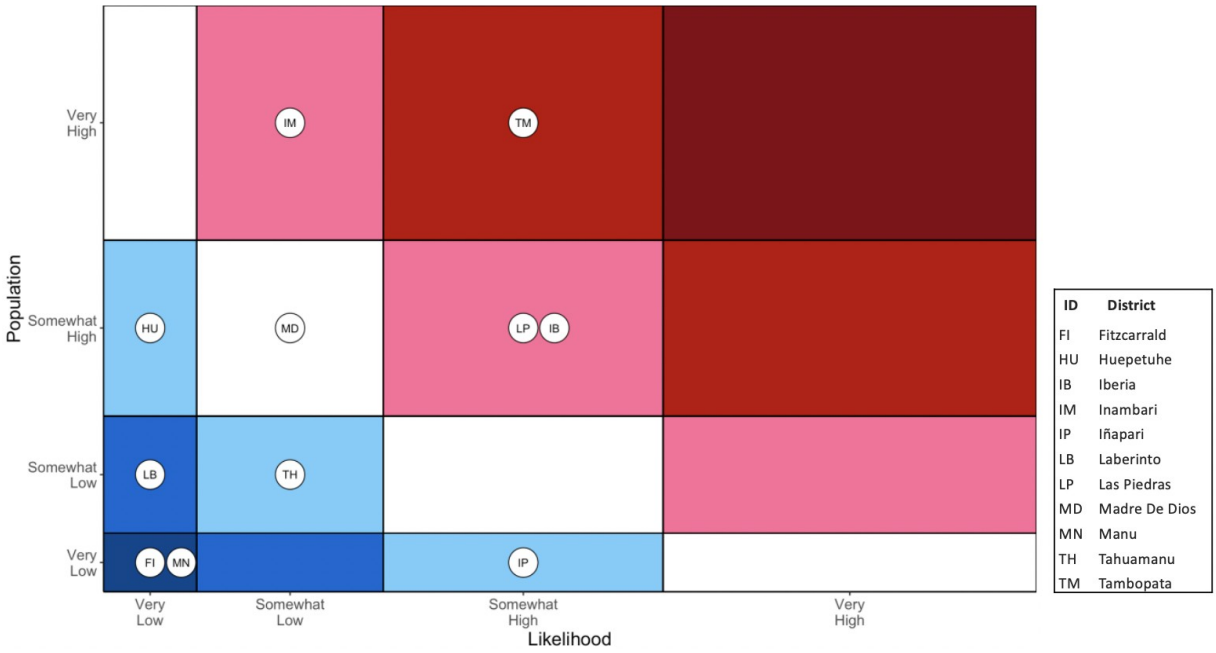

Figure 3. Risk matrix for dengue fever for the 2010 seasonal year. Here, circles represent districts, denoted by their ID, plotted according to likelihood and population size. The color represents the intensity of risk.

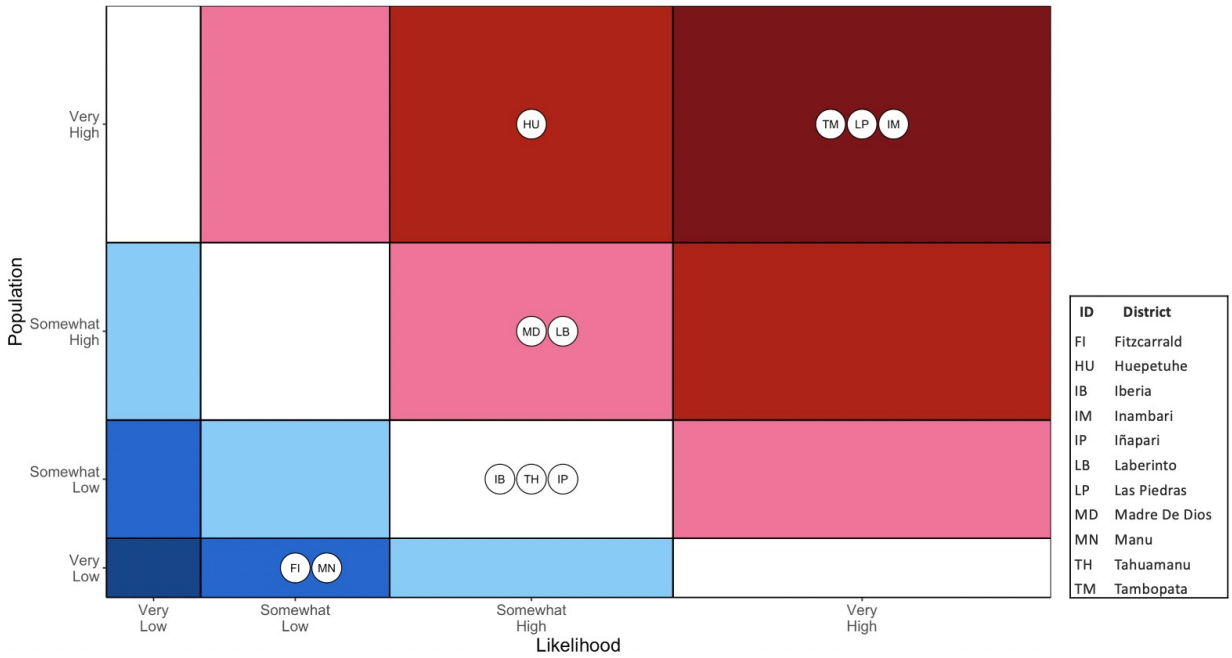

Figure 4. Risk matrix for dengue fever for the 2020 seasonal year.

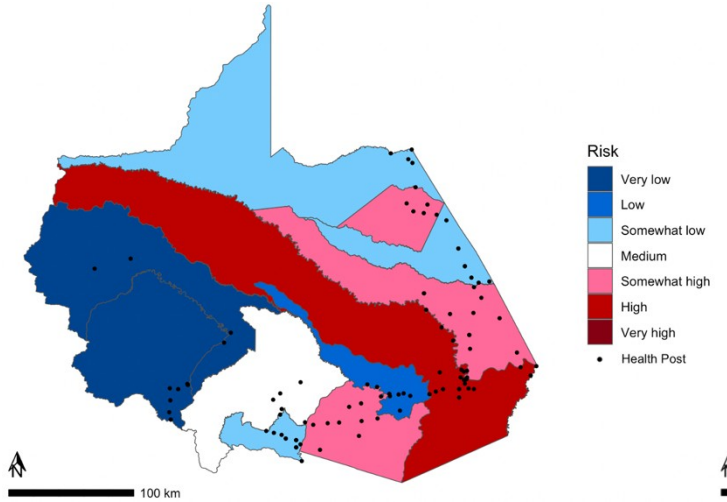

Figure 5. Risk map for dengue fever for 2010.

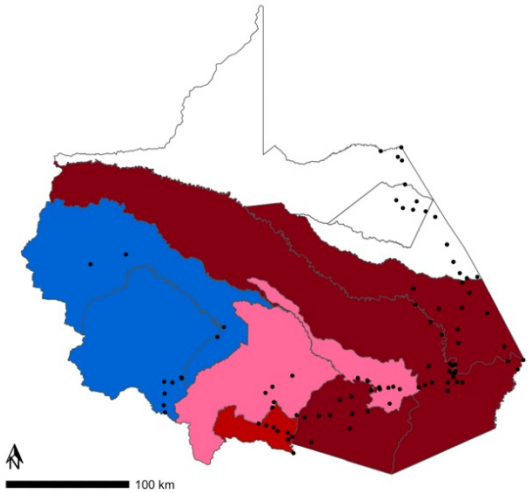

Figure 6. Risk map for dengue fever for 2020.

Table 5.
Total dengue fever cases for the 2010 and 2020 seasonal year.

District	District Risk 2010	Total Incidence 2010	District Risk 2020	Total Incidence 2020
Tambopata	High	1371	Very High	4315
Inambari	Somewhat High	43	Very High	1057
Las Piedras	Somewhat High	32	Very High	1028
Laberinto	Low	62	Somewhat High	390
Huepetuhe	Somewhat Low	42	High	377
Madre de Dios	Medium	6	Somewhat High	364
Iberia	Somewhat High	145	Medium	296
Iñapari	Somewhat Low	24	Medium	200
Tahuamanu	Somewhat Low	7	Medium	150
Manu	Very Low	0	Low	26
Fitzcarrald	Very Low	1	Low	0

4.3 Limitations

Our work provides a framework for analysis rather than a comprehensive tool due to limitations around temporal parameters, access to high-resolution data, and results that undervalue established predictors of these diseases. In regard to temporal parameters, we divided the disease incidence data into wet and dry seasons, using almanac dates from the literature. In reality, seasonal changes occur gradually over a period of time. Significantly more satellite images were

available for the wet season than for the dry season. This partially impacted our climatic variables, especially temperature data, which was inaccurate by several degrees. We did not include temperature in our model but acknowledge that it is an important factor to vector breeding and should be included in future models. In the R script, we left an option for partners to incorporate temperature into the risk matrix using externally acquired data.

Regarding low data resolution, we used data aggregated to a district level, which obscures local nuance. We could not use the finer-scale health data provided by MINSA because of the way disease is reported. Many of the cases recorded at health posts were contracted outside the district in which the health post is located. Cases in the Madre de Dios region often go unreported, further preventing an accurate landscape analysis of disease incidence. Our climatic and LULC variable data were similarly coarse. GPM IMERG has a resolution of 11 kilometers, which cannot represent local variation and increases error potential. We also identified a potential case of error in our LULC data, since the literature suggests that water is important for vector habitat but showed no significance in our model. The resolution of our LULC classification data may have also hidden significant trends for water, as our regression models did not reflect the importance of this variable for vector habitat.

Furthermore, the risk matrices we produced are also considered low resolution since they encompass large areas. Therefore, they should be used to inform, and not drive, decision making. We were also unable to integrate leishmaniasis into our risk matrices and risk maps as there were too many uncertain factors to consider in the framework of this project. It was not within our capacity to incorporate the lag period of 8 months between the climatic phenomenon in which leishmaniasis vectors breed and the actual transmission to humans.

4.4 Future Work

This project's limitations could be addressed with future work. Successive researchers can build upon our findings by using higher-resolution satellite data and more detailed health data. PeruSAT imagery, which has a resolution of 3 meters, could create a more detailed, accurate LULC classification and allow for the inclusion of additional land types (*Figure* D1). Illegal mining, especially, is an important LULC variable that merits further analysis using high-resolution remote sensing data since it is one of the most common causes of habitat disruption, especially on indigenous lands. Researchers could utilize data from IBC to analyze disease risk in relation to proximity to sovereign territory. Researchers could also integrate higher-resolution satellite data to conduct more precise analyses for temperature and precipitation variables, since our team was not able to access accurate temperature data and had to use scaled precipitation data to match precipitation intervals established in the literature. After researchers have conducted more in-depth analysis around environmental variables, higher-resolution health data at the address-scale can be used to assess the source of disease incidence at the community level and the status of health infrastructure (e.g., staffing and medication availability). Researchers should also acquire data for and apply this process to leishmaniasis, as our team did not have the resources necessary to study the disease. Future studies should focus on evaluating which variables increase outbreak risk in areas with high incidences of leishmaniasis.

5. Conclusions

Ultimately, our team created a streamlined process to explain dengue fever risk with climatic, topographic, and LULC variables and visualize this risk at a district level overlaid by health post locations. Through analyzing these variables individually and in combination with one another, we identified urban-forest edge area, urban area, precipitation range, and slope range as the model with the highest correlation for dengue incidence. According to the risk matrix and risk map we created, the districts of Tambopata, Las Piedras, and Inambari were at higher risk for disease transmission in both 2010 and 2020. Our methods of analysis, results, and visualizations will serve as a framework for further exploration into higher-resolution climatic data and more land-use change variables based on partners' observations on the ground. Moreover, as zoonotic disease incidence continues to rise in Madre de Dios, MINSA, MINAM, and our collaborating partners can utilize our products to inform their decision making. The risk matrix and risk map script, along with our more general research findings, can help them direct resources to vulnerable districts and advocate for policy changes which can address the environmental variables amplifying risk. Additionally, this project exemplified the importance of interdisciplinary collaboration across academic, governmental, and non-profit organizations in addressing planetary health.

6. Acknowledgments

We would like to thank our partners for their valuable support: César Munayco with MINSA; Tatiana Pequeño, William Augusto Llactayo Leon, and Germán Marchand with MINAM; Ellen Delgado Florian, Dr. Armando Valdez-Vasquez, Gabriel Carrasco, Viviana Sanchez-Aizcorbe Hennings, and Camila Llarena Cayo, with The Lab for EcoHealth and Urban Ecology at la Universidad Peruana Cayetano Heredia; Sidney Novoa and Judith Westveer with ACCA; Kathrin Hopfgartner and Andrea Bravo with IBC; and Jose Pasapera Gonzales with CONIDA. In addition, we would like to thank our science advisors, Dr. Marguerite Madden and Dr. Xiao Feng, as well as our DEVELOP Fellow, Sarah Payne, for their tremendous support and mentorship.

Any opinions, findings, and conclusions or recommendations expressed in this material are those of the author(s) and do not necessarily reflect the views of the National Aeronautics and Space Administration.

This material is based upon work supported by NASA through contract NNL16AA05C.

7. Glossary

Dengue Fever – A viral tropical mosquito-borne disease
Endemic – Restricted in location to a native habitat
ETM+ – Enhanced Thematic Mapper Plus
GPM – Global Precipitation Measurement
Health Posts – Local medical clinics
IMERG – Integrated Multi-satellitE Retrievals for GPM
Incidence – The occurrence of new cases within a set time frame
Leishmaniasis – A sandfly-borne parasitic disease

LST – Land Surface Temperature
SRTM – Shuttle Radar Topography Mission
Zoonotic Disease – A disease transferred to people from animals

8. References

Borges, D., Cesario, M., Rangel Cesario, R., Chauca, J. M., Garcia-Zapata, T. A., Gotuzzo, E., Guerra, H., Murto, C., Pinto, M., Schelling, E., & Ventosilla, P. (2015). Migration and the ecology of American Cutaneous Leishmaniasis in Madre de Dios, Peru, and Acre, Brazil: A mixed methods approach. [Working paper]. *Swiss Network for International Studies.* https://snis.ch/projects/integrated-analyses-of-human-dimensions-and-policy-implications-of-cross-border-migration-on-vector-borne-neglected-tropical-diseases-ntds-in-the-andes-amazon-region/

Charette, M., Berrang-Ford, L., Coomes, O., Llanos-Cuentas, E. A., Cárcamo, C., Kulkarni, M., & Harper, S. L. (2020). Dengue Incidence and Sociodemographic Conditions in Pucallpa, Peruvian Amazon: What Role for Modification of the Dengue–Temperature Relationship? *The American Journal of Tropical Medicine and Hygiene*, *102*(1), 180–190. https://doi.org/10.4269/ajtmh.19-0033

Chowell, G., Torre, C. A., Munayco-Escate, C., Suárez-Ognio, L., López-Cruz, R., Hyman, J. M., & Castillo-Chavez, C. (2008). Spatial and temporal dynamics of dengue fever in Peru: 1994–2006. *Epidemiology and Infection*, *136*(12), 1667–1677. https://doi.org/10.1017/S0950268808000290

Gambino, C., Beaudry, B., Berman, M., & Colmenares, M. (2019). Southern Maine Health & Air Quality. Examining Tick-Borne Illness Risk by Evaluating Land Cover and Tick Habitat Suitability in Southern Maine [Unpublished manuscript]. MA Node, NASA DEVELOP.

Guagliardo, S. A., Morrison, A. C., Barboza, J. L., Requena, E., Astete, H., Vazquez-Prokopec, G., & Kitron, U. (2015) River Boats Contribute to the Regional Spread of the Dengue Vector Aedes aegypti in the Peruvian Amazon. *PLoS Neglected Tropical Diseases 9*(4), Article e0003648. https://doi.org/10.1371/journal.pntd.0003648

Huffman, G. J., Stocker, E. F., Bolvin, D. T., Nelkin, E. J., & Tan, J. (2019). GPM IMERG Final Precipitation L3 Half Hourly 0.1 degree x 0.1 degree V06 [Data set]. Greenbelt, MD, Goddard Earth Sciences Data and Information Services Center (GES DISC). https://doi.org/10.5067/GPM/IMERG/3B-HH/06

Jarvis, A., Reuter, H. I., Nelson, A., & Guevara, E. (2008). Hole-filled SRTM for the globe Version 4, available from the CGIAR-CSI SRTM 90m [Data set]. Database: https://srtm.csi.cgiar.org. https://doi.org/10.5066/F7K072R7

Lana, J. T., Mallipudi, A., Ortiz, E. J., Arevalo, J. H., Llanos-Cuentas, A., & Pan, W. K. (2021). Risk factors for cutaneous leishmaniasis in a high-altitude forest region of Peru. *Tropical Medicine and Health*, *49*(1), Article 40. https://doi.org/10.1186/s41182-021-00332-0

Nicolau, A. P., Herndon, K., Flores-Anderson, A., & Griffin, R. (2019). A spatial pattern analysis of forest loss in the Madre de Dios region, Peru.

Environmental Research Letters, *14*(12), Article 124045. https://doi.org/10.1088/1748-9326/ab57c3

Okwor, I., & Uzonna, J. (2016). Social and economic burden of human leishmaniasis. *The American Journal of Tropical Medicine and Hygiene*, *94*(3), 489–493. https://doi.org/10.4269/ajtmh.15-0408

Purse, B. V., Masante, D., Golding, N., Pigott, D., Day, J. C., Ibañez-Bernal, S., Kolb, M., & Jones, L. (2017). How will climate change pathways and mitigation options alter incidence of vector-borne diseases? A framework for leishmaniasis in South and Meso-America. *PLoS ONE*, *12*(10), Article e0183583. https://doi.org/10.1371/journal.pone.0183583

Romero, G. A. S., & Boelaert, M. (2010). Control of visceral leishmaniasis in Latin America—A systematic review. *PLoS Neglected Tropical Diseases*, *4*(1), 1–17. https://doi.org/10.1371/journal.pntd.0000584

Salami, D., Sousa, C. A., Martins, M. R. O., & Capinha, C. (2020). Predicting dengue importation into Europe, using machine learning and model-agnostic methods. *Scientific Reports*, *10*, Article 9689. https://doi.org/10.1038/s41598-020-66650-1

Salmón-Mulanovich, G., Blazes, D. L., Guezala V, M. C., Rios, Z., Espinoza, A., Guevara, C., Lescano, A. G., Montgomery, J. M., Bausch, D. G., & Pan, W. K. (2018). Individual and spatial risk of dengue virus infection in Puerto Maldonado, Peru. *The American Journal of Tropical Medicine and Hygiene*, *99*(6), 1440–1450. https://doi.org/10.4269/ajtmh.17-1015

Stapleton, E., Calle, A., Chacon, N., Huffaker, N., & Nguyen, O. (2021). Peru Health and Air Quality: Land Use Change in the Rapidly Developing Peruvian Amazon and Implications on Zoonotic Disease Incidence [Unpublished manuscript]. GA Node, NASA DEVELOP.

Tsheten, T., Clements, A. C. A., Gray, D. J., & Wangdi, K. (2021). Dengue risk assessment using multicriteria decision analysis: A case study of Bhutan. *PLoS Neglected Tropical Diseases*, *15*(2), Article e0009021. https://doi.org/10.1371/journal.pntd.0009021

US Geological Survey Earth Resources Observation and Science Center. Landsat 4-5 TM [Data set]. US Geological Survey. https://doi.org/10.5066/F7N015TQ

US Geological Survey Earth Resources Observation and Science Center. Collection 2 Landsat 7 Enhanced Thematic Mapper Plus (ETM+) Level-2 Science Product [Data set]. US Geological Survey. https://doi.org/10.5066/P9C7I13B

US Geological Survey Earth Resources Observation and Science Center. Collection 2 Landsat 8-9 Operational Land Imager (OLI) and Thermal Infrared Sensor (TIRS) Level-2 Science Product [Data set]. US Geological Survey. https://dx.doi.org/10.5066/P9OGBGM6

Wimberley, M. K., de Beurs, K. M., Loboda, T. V., & Pann, W. K. (2021). Satellite observations and malaria: New opportunities for research and applications. *Trends in Parasitology*, *7*(6), 525–537. https://doi.org/10.1016/j.pt.2021.03.003

World Health Organization. (2021, May 20). *Leishmaniasis.* https://www.who.int/news-room/fact-sheets/detail/leishmaniasis

Yanoviak, S. P., Paredes, J. E. R., Lounibos, L. P., & Weaver, S. C. (2006). Deforestation alters phytotelm habitat availability and mosquito production in the Peruvian Amazon. *Ecological Applications*, *16*(5), 1854–1864. https://doi.org/10.1890/1051-0761(2006)016[1854:DAPHAA]2.0.CO;2

9. Appendices

Appendix A

Table A1
Regression Variables

Category	Variable	Units	Parameters
Climatic	Temperature	Celsius	Minimum, maximum, mean, median, and range
Climatic	Precipitation	Millimeters	Minimum, maximum, mean, median, and range
Topographic	Elevation	Meters	Minimum, maximum, mean, median, and range
Topographic	Slope	Degrees	Minimum, maximum, mean, median, and range
LULC	Urban Area	Kilometers-squared	Area (km^2) and percent total area (%)
LULC	Forest Area	Kilometers-squared	Area (km^2) and percent total area (%)
LULC	Agriculture and Pastures	Kilometers-squared	Area (km^2) and percent total area (%)
LULC	Water and Wetlands	Kilometers-squared	Area (km^2) and percent total area (%)
LULC	Human-Altered Environments (Urban, Agriculture, Pastures, Mining)	Kilometers-squared	Area (km^2) and percent total area (%)
LULC	Urban Edge	Kilometers-squared	Area (km^2) and percent total area (%)
LULC	Forest Edge	Kilometers-squared	Area (km^2) and percent total area (%)
LULC	Urban-Forest Edge	Kilometers-squared	Area (km^2) and percent total area (%)

Appendix B

Table B1

Land Use & Land Change Variables for Dengue Fever

LULC	Wet Season 2010	Seasonal Year 2010	Wet Season 2020	Seasonal Year 2020
Urban (km^2)	$R^2 = 0.3725$	$R^2 = 0.3628$	$R^2 = 0.1681$	$R^2 = 0.1763$
	$\rho = 0.0272$	$\rho = 0.02934$	$\rho = 0.1162$	$\rho = 0.1101$
Urban (% area)	$R^2 = 0.3908$	$R^2 = 0.3597$	$R^2 = 0.07291$	$R^2 = 0.07275$
	$\rho = 0.02348$	$\rho = 0.03007$	$\rho = 0.2142$	$\rho = 0.2144$
Forest (km^2)	$R^2 = -0.06705$	$R^2 = -0.04187$	$R^2 = -0.0867$	$R^2 = -0.08694$
	$\rho = 0.5572$	$\rho = 0.4591$	$\rho = 0.6636$	$\rho = 0.6652$
Forest (% area)	$R^2 = -0.09992$	$R^2 = -0.1091$	$R^2 = -0.06992$	$R^2 = -0.06814$
	$\rho = 0.769$	$\rho = 0.9002$	$\rho = 0.5706$	$\rho = 0.5622$
Water (km^2)	$R^2 = -0.03127$	$R^2 = -0.04615$	$R^2 = -0.08595$	$R^2 = -0.0824$
	$\rho = 0.4255$	$\rho = 0.4738$	$\rho = 0.6587$	$\rho = 0.6372$
Water (% area)	$R^2 = -0.1086$	$R^2 = -0.1067$	$R^2 = 0.001778$	$R^2 = 0.005357$
	$\rho = 0.8994$	$\rho = 0.8539$	$\rho = 0.3394$	$\rho = 0.3314$
Agriculture & Pastures (km^2)	$R^2 = 0.1728$	$R^2 = 0.1435$	$R^2 = 0.0009191$	$R^2 = 0.004935$
	$\rho = 0.1127$	$\rho = 0.1363$	$\rho = 0.3413$	$\rho = 0.3323$
Agriculture & Pastures (% area)	$R^2 = 0.1847$	$R^2 = 0.1077$	$R^2 = 0.1772$	$R^2 = 0.1768$
	$\rho = 0.1043$	$\rho = 0.1715$	$\rho = 0.2095$	$\rho = 0.1098$
Human-Altered Environments (km^2)	$R^2 = 0.1085$	$R^2 = 0.09278$	$R^2 = 0.0578$	$R^2 = 0.06562$
	$\rho = 0.1706$	$\rho = 0.1887$	$\rho = 0.2359$	$\rho = 0.2244$
Human-Altered Environments (% area)	$R^2 = -0.07558$	$R^2 = -0.07913$	$R^2 = -0.05715$	$R^2 = -0.05707$
	$\rho = 0.5988$	$\rho = 0.618$	$\rho = 0.515$	$\rho = 0.5146$

Table B2

Edge Variables for Dengue Fever

Edge	Wet Season 2010	Seasonal Year 2010	Wet Season 2020	Seasonal Year 2020
Urban-Forest Edge (km^2)	$R^2 = 0.5389$	$R^2 = 0.5536$	$R^2 = 0.2235$	$R^2 = 0.2167$
	$\rho = 0.006$	$\rho = 0.005229$	$\rho = 0.08044$	$\rho = 0.08422$
Urban-Forest Edge (%)	$R^2 = 0.3008$	$R^2 = 0.3044$	$R^2 = 0.04028$	$R^2 = 0.03536$
	$\rho = 0.04681$	$\rho = 0.04559$	$\rho = 0.2639$	$\rho = 0.2724$
Urban-Edge (km^2)	$R^2 = 0.39$	$R^2 = 0.378$	$R^2 = 0.1745$	$R^2 = 0.1835$
	$\rho = 0.0236$	$\rho = 0.02604$	$\rho = 0.1113$	$\rho = 0.1051$
Urban-Edge (%)	$R^2 = 0.3579$	$R^2 = 0.3309$	$R^2 = 0.05378$	$R^2 = 0.05375$
	$\rho = 0.03048$	$\rho = 0.03747$	$\rho = 0.242$	$\rho = 0.2421$
Forest-Edge	$R^2 = -0.04324$	$R^2 = -0.0562$	$R^2 = -0.0496$	$R^2 = -0.05764$

(km^2)	ρ = 0.4637	ρ = 0.5112	ρ = 0.4861	ρ = 0.5169
Forest-Edge (%)	R^2 = -0.1099	R^2 = -0.1081	R^2 = -0.1108	R^2 = -0.111
	ρ = 0.9221	ρ = 0.8791	ρ = 0.9589	ρ = 0.9816

Table B3
Topographic Variables for Dengue Fever

Topographic	Wet Season 2010	Seasonal Year 2010	Wet Season 2020	Seasonal Year 2020
Elevation Minimum	R^2 = 0.02229	R^2 = -0.03178	R^2 = 0.3845	R^2 = 0.3836
	ρ = 0.2965	ρ = 0.427	ρ = 0.02472	ρ = 0.02489
Elevation Maximum	R^2 = 0.3039	R^2 = 0.2957	R^2 = 0.3545	R^2 = 0.3375
	ρ = 0.04575	ρ = 0.04857	ρ = 0.03131	ρ = 0.03566
Elevation Median	R^2 = 0.05133	R^2 = 0.0004743	R^2 = 0.6426	R^2 = 0.6307
	ρ = 0.2458	ρ = 0.3424	ρ = 0.001832	ρ = 0.002136
Elevation Mean	R^2 = 0.1224	R^2 = 0.09355	R^2 = 0.50787	R^2 = 0.4879
	ρ = 0.1561	ρ = 0.1878	ρ = 0.008337	ρ = 0.01008
Elevation Range	R^2 = 0.3022	R^2 = 0.2975	R^2 = 0.338	R^2 = 0.3211
	ρ = 0.04531	ρ = 0.04793	ρ = 0.03551	ρ = 0.04032
Slope Maximum	R^2 = 0.4059	R^2 = 0.4023	R^2 = 0.4704	R^2 = 0.4587
	ρ = 0.02076	ρ = 0.02138	ρ = 0.01186	ρ = 0.01318
Slope Median	R^2= -0.02949	R^2 = -0.06441	R^2 = 0.3423	R^2 = 0.3375
	ρ = 0.4202	ρ = 0.5454	ρ = 0.03438	ρ = 0.03566
Slope Mean	R^2 = 0.1218	R^2 = 0.08032	R^2 = 0.4167	R^2 = 0.4022
	ρ = 0.1568	ρ = 0.2043	ρ = 0.01897	ρ = 0.0214
Slope Range	R^2 = 0.4059	R^2 = 0.4023	R^2 = 0.4704	R^2 = 0.4587
	ρ = 0.02076	ρ = 0.02138	ρ = 0.01186	ρ = 0.01318

Table B4
Precipitation Variables for Dengue Fever

Precipitation	Wet Season 2010	Seasonal Year 2010	Wet Season 2020	Seasonal Year 2020
Precipitation Minimum	R^2= -0.0589	R^2= -0.07084	R^2= -0.104	R^2= -0.1024
	ρ = 0.52	ρ = 0.575	ρ = 0.8148	ρ = 0.7959
Precipitation Maximum	R^2= 0.3152	R^2=0.3086	R^2= 0.06081	R^2= 0.0569
	ρ = 0.04213	ρ = 0.0442	ρ = 0.221	ρ = 0.2372
Precipitation Mean	R^2= -0.1055	R^2= -0.1042	R^2= -0.1088	R^2= -0.1083
	ρ = 0.8354	ρ = 0.8171	ρ = 0.8947	ρ = 0.8831
Precipitation Median	R^2= -0.09728	R^2= -0.1035	R^2= -0.08331	R^2= -0.08007
	ρ = 0.744	ρ = 0.8087	ρ = 0.6423	ρ = 0.6233
Precipitation	R^2= 0.3153	R^2= 0.3084	R^2= 0.06715	R^2= 0.05632

Range	ρ = 0.04209	ρ = 0.04427	ρ = 0.2222	ρ = 0.2381

Appendix C

Table C1

Land Use & Land Change Variables for Leishmaniasis

LULC	Wet Season 2010	Seasonal Year 2010	Wet Season 2020	Seasonal Year 2020
Urban (km^2)	R^2 = 0.03552	R^2 = 0.09198	R^2 = -0.1024	R^2 = -0.09027
	ρ = 0.2722	ρ = 0.1896	ρ = 0.7957	ρ = 0.688
Urban (% area)	R^2 = -0.1058	R^2 = -0.08144	R^2 = -0.08829	R^2 = -0.09301
	ρ = 0.8404	ρ = 0.6311	ρ = 0.6742	ρ = 0.7084
Forest (km^2)	R^2 = -0.07692	R^2 = -0.0794	R^2 = -0.1001	R^2 = -0.08193
	ρ = 0.6059	ρ = 0.6175	ρ = 0.7705	ρ = 0.634
Forest (% area)	R^2 = -0.07734	R^2 = -0.0414	R^2 = -0.1111	R^2 = -0.1078
	ρ = 0.6082	ρ = 0.4576	ρ = 0.985	ρ = 0.8736
Water (km^2)	R^2 = 0.158	R^2 = 0.1731	R^2 = 0.1111	R^2 = -0.08707
	ρ = 0.1241	ρ = 0.1125	ρ = 0.9926	ρ = 0.666
Water (% area)	R^2 = 0.14	R^2 = 0.1678	R^2 = -0.1091	R^2 = -0.08762
	ρ = 0.1394	ρ = 0.1165	ρ = 0.9016	ρ = 0.6697
Agriculture & Pastures (km^2)	R^2 = 0.1493	R^2 = 0.1788	R^2 = -0.08292	R^2 = -0.04966
	ρ = 0.1314	ρ = 0.1084	ρ = 0.6399	ρ = 0.4863
Agriculture & Pastures (% area)	R^2 = -0.002128	R^2 = 0.03572	R^2 = -0.07878	R^2 = -0.0857
	ρ = 0.3483	ρ = 0.2718	ρ = 0.6161	ρ = 0.6572
Human-Altered Environments (km^2)	R^2 = 0.1832	R^2 = 0.2476	R^2 = -0.0776	R^2 = -0.03927
	ρ = 0.1053	ρ = 0.0682	ρ = 0.6096	ρ = 0.4505
Human-Altered Environments (% area)	R^2 = -0.1086	R^2 = -0.09222	R^2 = -0.07851	R^2 = -0.07688
	ρ =0.8905	ρ = 0.7024	ρ = 0.6145	ρ = 0.6057

Table C2

Edge Variables for Leishmaniasis

Edge	Wet Season 2010	Seasonal Year 2010	Wet Season 2020	Seasonal Year 2020
Urban-Forest Edge (km^2)	R^2 = -0.07998	R^2 = -0.02922	R^2 = 0.06285	R^2 = 0.05536
	ρ = 0.6228	ρ = 0.4193	ρ = 0.2284	ρ = 0.2396
Urban-Forest Edge (%)	R^2 = -0.1093	R^2 = -0.1083	R^2 = -0.03444	R^2 = -0.05339
	ρ = 0.9053	ρ = 0.883	ρ = 0.4352	ρ = 0.5003
Urban-Edge (km^2)	R^2 = 0.02514	R^2 = 0.08487	R^2 = -0.1058	R^2 = -0.09648
	ρ = 0.2911	ρ = 0.1984	ρ = 0.8406	ρ = 0.7369
Urban-Edge (%)	R^2 = -0.1088	R^2 = -0.08931	R^2 = -0.09032	R^2 = -0.09438
	ρ = 0.89450	ρ = 0.6812	ρ = 0.6884	ρ = 0.7193
Forest-Edge (km^2)	R^2 = 0.05229	R^2 = 0.04496	R^2 = 0.07705	R^2 = -0.03265
	ρ = 0.2443	ρ = 0.2561	ρ = 0.2086	ρ = 0.4296

Forest-Edge (%)	R^2 = 0.007352	R^2 = 0.01721	R^2 = -0.04756	R^2 = -0.08351
	ρ = 0.3271	ρ = 0.3065	ρ = 0.4788	ρ = 0.6435

Table C3
Topographic Variables for Leishmaniasis

Topographic	Wet Season 2010	Seasonal Year 2010	Wet Season 2020	Seasonal Year 2020
Elevation Minimum	R^2 = 0.57	R^2 = 0.5849	R^2 = 0.04997	R^2 = 0.07271
	ρ = 0.004379	ρ = 0.003705	ρ = 0.248	ρ = 0.2144
Elevation Maximum	R^2 = 0.1554	R^2 = 0.2188	R^2 = 0.1887	R^2 = 0.07565
	ρ = 0.1262	ρ = 0.08302	ρ = 0.1015	ρ = 0.2105
Elevation Median	R^2 = 0.6872	R^2 = 0.698	R^2 = 0.309	R^2 = 0.2402
	ρ = 0.0009843	ρ = 0.0008354	ρ = 0.04408	ρ = 0.07179
Elevation Mean	R^2 = 0.7461	R^2 = 0.7387	R^2 = 0.6239	R^2 = 0.5015
	ρ = 0.0003744	ρ = 0.000427	ρ = 0.002329	ρ = 0.008863
Elevation Range	R^2 = 0.136	R^2 = 0.198	R^2 = 0.1841	R^2 = 0.06955
	ρ = 0.1431	ρ = 0.09546	ρ =0.1046	ρ = 0.2188
Slope Maximum	R^2 = 0.1049	R^2 = 0.2298	R^2 = 0.06377	R^2 = -0.04123
	ρ = 0.1747	ρ =0.07707	ρ = 0.227	ρ = 0.457
Slope Median	R^2= 0.5659	R^2 = 0.5038	R^2 = 0.1334	R^2 = 0.1072
	ρ = 0.004578	ρ = 0.008662	ρ = 0.1455	ρ = 0.1721
Slope Mean	R^2 = 0.6443	R^2 = 0.6002	R^2 = 0.3495	R^2 = 0.2577
	ρ = 0.001791	ρ = 0.003102	ρ = 0.03254	ρ = 0.06358
Slope Range	R^2 = 0.1049	R^2 = 0.2298	R^2 = 0.06377	R^2 = -0.04123
	ρ = 0.1747	ρ = 0.7707	ρ = 0.227	ρ = 0.457

Table C4
Precipitation Variables for Leishmaniasis

Precipitation	Wet Season 2010	Seasonal Year 2010	Wet Season 2020	Seasonal Year 2020
Precipitation Minimum	R^2= -0.07497	R^2= -0.1108	R^2= -0.078	R^2= -0.09408
	ρ = 0.5956	ρ = 0.9617	ρ = 0.6117	ρ = 0.7168
Precipitation Maximum	R^2= -0.1107	R^2= 0.01717	R^2= -0.1081	R^2= -0.1051
	ρ = 0.9542	ρ = 0.3066	ρ = 0.8794	ρ = 0.8301
Precipitation Mean	R^2= -0.07109	R^2= -0.05803	R^2= -0.1047	R^2= -0.1061
	ρ = 0.5762	ρ = 0.5185	ρ = 0.8247	ρ = 0.8438
Precipitation Median	R^2= -0.06818	R^2= -0.1076	R^2= -0.09205	R^2= -0.1051
	ρ = 0.5624	ρ = 0.8703	ρ = 0.7011	ρ = 0.8301
Precipitation Range	R^2= -0.1108	R^2= 0.01665	R^2= -0.1077	R^2= -0.1056
	ρ = 0.964	ρ = 0.3077	ρ = 0.8712	ρ = 0.8377

Appendix D

Figure D1. Puerto Maldonado PeruSAT imagery in 2021 vs Landsat 8 OLI imagery in 2020.